February 2024
Master's Degree Thesis

Smart Ride-Through Control of a PV Microgrid System under Voltage Faults

Graduate School of Chosun University

Department of Electrical Engineering

Muhammad Affan Khan

Smart Ride-Through Control of a PV Microgrid System under Voltage Faults

전압 결함이 있는 태양광 마이크로그리드
시스템의 지능형 라이드 스루 제어

February 23, 2024

Graduate School of Chosun University

Department of Electrical Engineering

Muhammad Affan Khan

Smart Ride-Through Control of a PV Microgrid System under Voltage Faults

Advisor: Jaehong Kim

A dissertation submitted in partial fulfillment of the requirements for a Master's Degree

October 2023

Graduate School of Chosun University

Department of Electrical Engineering

Muhammad Affan Khan

Muhammad Affan Khan's Master Thesis

Approved

Committee Chairman	Yong-Jae Kim	(인)
Committee Member	Youn-Ok Choi	(인)
Committee Member	Jaehong Kim	(인)

December 2023

Graduate School of Chosun University

TABLE OF CONTENTS

LIST OF ABBREVIATIONS AND ACRONYMS

PV	Photovoltaic
GCPV	Grid-Connected Photovoltaic
LVRT	Low-Voltage Ride-Through
NN	Neural Network
DG	Distributed Generation
MPPT	Maximum Power Point Tracking
PR	Proportional Resonant
PI	Proportional Integral
PLL	Phase-Locked-Loop
SRF	Synchronous Reference Frame
VSI	Voltage Source Inverter
RMS	Root Mean Square
ANN	Artificial Neural Network
MSE	Mean Squared Error
PCC	Point of Common Coupling
PSO	Particle Swarm Optimization
CSS	Current Saturation Strategy

List of Figures

List of Tables

ABSTRACT

Smart Ride-Through control of a PV Microgrid System under Voltage Faults

Muhammad Affan Khan
Advisor: Prof. Jaehong Kim, Ph.D.
Department of Electrical Engineering
Graduate School of Chosun University

The proliferation of photovoltaic low power distributed generators in modern grids raises concerns about grid stability. To address this, network operators must periodically update grid codes, especially with the widespread adoption of grid-connected photovoltaic systems (GCPVs). Integrating renewable energy sources, such as photovoltaic systems, into large-scale electrical grids faces challenges in withstanding low voltage phases (LVRT). Recent grid code advancements require distributed generation resources to withstand grid faults. This study investigates these destabilizing conditions of fault through different simulations of a PV microgrid system. It employs a dc-chopper circuit, that manages dc-link over-voltage and maintenance of current within acceptable limits per standards is also carried out. The primary contribution is a framwork of neural network (NN) control that detects voltage sags with improved efficiency, understands their characteristics, and injects reactive current to meet grid code requirements. This NN model is systematically developed using data from diverse simulation scenarios. Compared to the RMS fault detection method and conventional LVRT algorithm, the NN control approach demonstrates superior accuracy and robustness, particularly in challenging sag scenarios.

국문초록

전압 결함이 있는 태양광 마이크로그리드 시스템의 지능형 라이드 스루 제어

칸 무함마드 아판
지도 교수: 김재홍
전기 공학과
조선대학교 대학원

현대 그리드에서 저전력 광전지 분산 발전기의 확산은 그리드 안정성에 대한 우려를 불러일으킵니다. 이 문제를 해결하려면 네트워크 운영자는 특히 GCPV(그리드 연결 태양광 발전 시스템)가 널리 채택됨에 따라 그리드 코드를 정기적으로 갱신해야 합니다. 광전지 시스템과 같은 재생 가능 에너지원을 대규모 전력망에 통합하는 것은 저전압 Ride-Through(LVRT)를 견디는 데 어려움을 겪습니다. 최근의 그리드 코드 발전에는 그리드 고장을 견딜 수 있는 분산 발전 리소스가 필요합니다. 본 연구에서는 PV 마이크로그리드 시스템의 다양한 시뮬레이션을 통해 이러한 불안정한 결함 조건을 조사합니다. DC 초퍼 회로를 사용하여 DC 링크 과전압을 관리하고 표준에 따라 허용 가능한 한도 내에서 전류를 유지합니다. 주요 기여는 전압 강하를 효과적으로 감지하고 그 특성을 이해하며 그리드 코드 요구 사항을 충족하기 위해 무효 전류를 주입하는 신경망(NN) 제어 프레임워크입니다. 이 NN 모델은 다양한 시뮬레이션 시나리오의 데이터를 사용하여 체계적으로 개발되었습니다. RMS 결함 감지 방법 및 기존 LVRT 알고리즘과 비교하여 NN 제어 접근 방식은 특히 까다로운 새그 시나리오에서 뛰어난 정확성과 강인성을 보여줍니다.

I. INTRODUCTION

A. Photovoltaic Microgrids

Over the last decade, there has been a significant rise in the number of grid systems using distributed generation (DG) units, such as photovoltaic (PV) systems. The reason for this increase is based on multiple advantages that these integrated systems provide, including low costs of energy generation, less carbon emissions, and higher reliability. One of the main benefits of microgrids is their ability to operate independently of the main grid. This means that they can provide electricity to communities that are not connected to the main grid or that experience frequent power outages. They can also provide backup power to critical infrastructure, such as hospitals and emergency response centers, in the event of a natural disaster or other emergency. Microgrids have an added advantage of incorporating renewable energy sources such as wind and solar power. These renewable resources are not continuously available as they are intermittent. However, microgrids can overcome this challenge by integrating energy storage technologies like batteries, ensuring the availability of electricity when needed, even during times when the sun is not shining or when the wind is not blowing.

The control system of a microgrid is a critical component that manages the flow of electricity within the system. It is responsible for monitoring the energy production and demand, and making decisions about when to use and store energy. The control system can also detect and respond to changes in the grid, such as fluctuations in voltage or frequency, and can isolate the microgrid from the main grid in the event of a disturbance. PV systems are designed to operate within a specific voltage range to maintain the stability of the entire microgrid and ensure normal operating conditions.

B. Literature Review

Over the past decade or so, there has been a significant increase in the prevalence of grid systems incorporating distributed generation (DG) units such as photovoltaic (PV) systems. This surge in their adoption can be attributed to the reason that these integrated systems offer several advantages, including low costs of energy generation, reduced carbon emissions, and higher reliability. These PV systems are ideally designed to function within a specified range of voltage to maintain the overall stability and normal operation of microgrids. However, the intermittent nature of energy generation by PV systems can potentially disrupt the seamless functioning of microgrids [1]. Consequently, operators of such networks must continually develop and revise grid codes to ensure the system remains stable. One of the most critical aspects of specified grid codes is the implementation of LVRT for PV microgrids [2]. LVRT is essentially a control mechanism that enables PV power generators to stay connected to the utility grid during short-term voltage dips or sags. Under typical operational conditions, PV systems operate at their maximum power point (MPP) and supply real power to grid. However, during LVRT events, PV power systems must inject reactive power into the grid to stabilize it and prevent disruptions [3].

The voltage versus time characteristics offer crucial insights into the Low Voltage Ride Through (LVRT) requirements. Essentially, these characteristics define the minimum duration for a system which can endure a specific level of voltage dip or sag. Figure 1 illustrates the minimum time span that a system must remain connected to the utility grid during voltage sag incidents, as mandated by grid codes in various countries. For a more accessible description of LVRT requirements, especially in alignment with German grid codes, the PV system should demonstrate its ability to endure voltage faults, including complete voltage sag (100% voltage sag), for a minimum of 0.15 seconds before disconnecting from the utility grid. In the case of Taiwan and Spain, their respective grid

codes specify a minimum limit of 0.5 seconds for voltage dips of 85% and 80%, respectively [2] (for this study, we are focusing on the grid code requirements outlined for Germany). LVRT stands as a critical requirement for ensuring the proper operation of the system and the uninterrupted supply of power to loads. In the event of a fault where more than one generating units disconnect, there is a risk of system breakdown, potentially leading to a blackout.

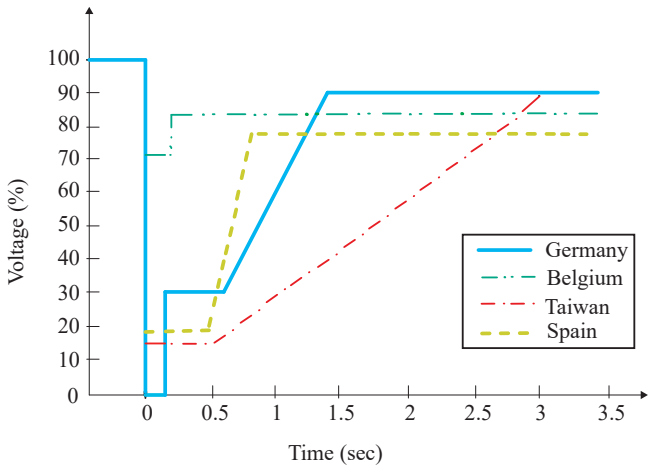

Figure 1: LVRT time period of different grid codes.

During the voltage ride-through process, two major issues that are addressed include dc-link over-voltage and reactive power injection. Reactive power injection is a highly effective technique to support the grid and to facilitate voltage recovery in the event of voltage sag faults. Numerous research papers have addressed the reduction of dc-link over-voltage and the control of current amplitude in PV inverters to protect them during voltage sags. In one instance [4], a dc-link adaptive voltage control method was employed to enhance the quality of the output waveform from PV inverters. This control strategy achieved the mitigation of dc-link over-voltage by dynamically adjusting the dc-link voltage. Another research study [5] proposed a control strategy that effectively managed both the over-current and the dc-link over-voltage during faults. In

a different approach [6], a proportional-resonant (PR) current controller has been implemented to limit over-current while simultaneously ensuring a high-quality sinusoidal output waveform. However, it's worth noting that none of the mentioned articles discussed the concept of injecting reactive power to support the grid during fault conditions.

Efficiently identifying voltage dip events is a critical aspect of low voltage ride-through capability. Recent literature has introduced several methods for detecting voltage dips, including the peak value detection method [7], the droop-control method [8], and the missing voltage method [9]. Among these recent methods, the root mean square (RMS) method [10] has proven to be the most effective. The RMS detection technique for voltage sag monitors the root mean square value of the (dq) coponents of grid voltage at the phase-locked-loop (PLL) stage. This technique measures the grid voltage (V_{gp}) at the current time.

Considering the need for dynamic voltage support, which involves injecting reactive power, various approaches have been employed to enhance the ability of microgrids to withstand voltage sag faults. Some of these methods utilize specialized devices, like active crowbar systems, energy storage systems [11], flexible AC transmission system devices (FACTS), brake choppers [12], dynamic voltage restorers (DVR), and fault current limiter (FCL) [13]. For instance, in the case of DVRs, a two-stage control design was proposed in [14] to insert reactive power into the grid and compensate for voltage sags. Another approach combines a supercapacitor-based energy storage system with a static synchronous compensator (STATCOM) as outlined in [15] to enhance low voltage ride-through (LVRT) capability. Such external devices play a crucial role in maintaining and stabilizing microgrid systems during voltage faults, but they do increase system cost and complexity. Therefore, there is a growing focus on improving LVRT with minimal cost through modifications to control algorithms and procedures. Recently, a new current saturation strategy (CSS)

[16] was introduced, demonstrating improved performance in enabling grid-forming inverters to ride through low-voltage events. Additionally, an enhanced particle swarm optimization (PSO)-based approach [17] has been applied to effectively manage LVRT in higher-power applications. Advanced neural networks, specifically neural network (NN) processing, have also been employed for optimal grid control under dynamic conditions, proving to be quite effective. In [18], authors presented the integration of NN-based control with conventional methods, enhancing grid behavior under real-world conditions and opening up new avenues for optimal power system control.

C. Thesis Objective

In this thesis, a PV-microgrid was designed and analyzed under voltage fault conditions. The system was equipped with low voltage ride-through capability, dc-link voltage limitation with the help of a dc-chopper circuit, ac over-current suppression, and reactive power injection using a proposed NN-based reactive current injection control. The NN-based control model efficiently analyzes grid voltage data to precisely identify voltage sags and capture their unique attributes. This initial capability ensures a thorough comprehension of sag occurrences. Following this, the NN model utilizes this sag data to offer essential grid assistance by accurately injecting the reactive current according to the requirements specified by grid codes.

The objectives obtained by this work are as mentioned above. This thesis is based on the research work carried out and also presented in an academic journal referenced as [19].

The thesis is organized in a manner that, literature review and objectives of the thesis are mentioned in Chapter I. Chapter II provides a detailed explanation of the system design, including its configurations. Chapter III focuses on the system's low voltage ride through capability. In Chapter IV, details about the

proposed NN-based control for LVRT are provided . The results obtained by the proposed controller are presented with comparision to the RMS sag detection and conventional LVRT control in Chapter V. Finally, the concluding remarks are given in Chapter VI.

II. Modelling of PV Microgrid System

The figure 2 illustrated depicts the PV microgrid system which includes a PV array that employs a maximum power point tracking (MPPT) technique. The PV array is controlled using the perturb & observe (P&O) method and is connected to a boost converter that is linked to a dc-chopper circuit. The dc-chopper circuit is used to manage any overvoltage at the dc-link stage. Furthermore, the system consists of a three-phase voltage source inverter (VSI) [20]. An RL filter is connected to the side having low-voltage of the step-up transformer, which is linked to the medium voltage side of the transformer that is in turn connected to the utility grid.

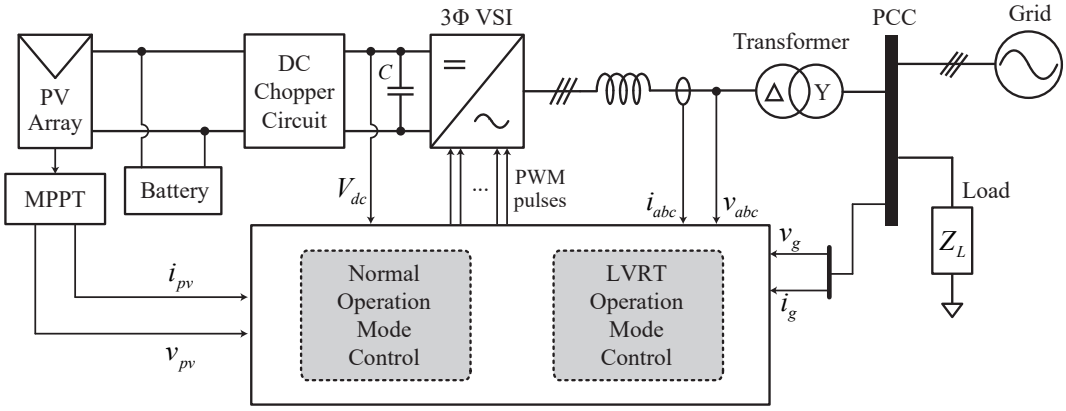

Figure 2: Configuration of PV microgrid system.

A. Equivalent circuit of PV module

Figure 3 shows the comparable diagram of a photovoltaic module, which comprises multiple solar cells. The connection between the output current and voltage of the module can be described using equation (1) given next [21]. The variables i_{Ph} and i_{sat} denote the photo current and the reverse saturation current of the module, respectively. The ideal factor of the diode is represented by m, and the Boltzmann constant is given by K. The electron charge is denoted by q, and

the equivalent parallel and series resistance of the module are represented by r_p and r_s, respectively.

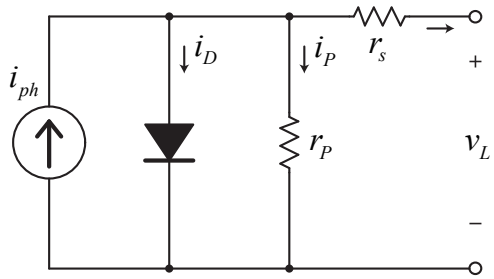

Figure 3: PV cell equivalent circuit.

$$i_L = i_{Ph} - i_{sat}\left[exp(\frac{qV_D}{mN_sKT}) - 1\right] - \frac{i_L r_S + v_L}{r_P}. \tag{1}$$

The equations (2)-(4) can be used to calculate the parameters of the equivalent circuit for a PV module based on the values of temperature (T_{ref}) and irradiation (G_{ref}). These parameters can also be used for the evaluation of the PV module. Equations taken from [21] and [22] can be used to calculate I_{ph} for any temperature and irradiation value, where I_{sc} denotes the nominal short circuit current. G and G_{ref} represent the actual and nominal irradiance, respectively, while T represents the temperature in kelvins and α_i represents the coefficient of current temperature.

$$i_{Ph} = [I_{sc} + \alpha_i(T - T_{ref})]\frac{G}{G_{ref}} \tag{2}$$

$$I_{sc} = I_{sc,ref}(\frac{r_P + r_S}{r_P}) \tag{3}$$

$$i_{sat} = \frac{I_{sc,ref} + \alpha_i(T - T_{ref})}{e^q(V_{oc,ref} + \alpha_v(T - T_{ref})/(N_s mKT) - 1} \tag{4}$$

Figure 4 displays the P-V and I-V characteristics of the PV module, which were generated in Simulink, with a standard temperature of T_{ref} = 25 °C and G_{ref} =

Table 2: PV module Parameters.

Parameters	Values	Parameters	Values
Maximum power voltage	V_{mp} = 29 V	Maximum power current	I_{mp}=7.35 A
Maximum power	P_{max}=213.15 W	Open circuit voltage	V_{oc}=36.3 V
Short circuit current	I_{sc}=7.84 A	Cells per module	N_{cell}=60
Temp. coefficient of V_{oc}	av = -0.367/°C	Temp. coefficient of I_{sc}	ai = 0.102/°C

1000 W/m^2.

B. PV array size and MPPT

Table 2 gives the parameters that are chosen for each of the 235 parallel strings from 16 modules to model the PV microgrid system. Each PV module is distributed having 235 parallel strings of 16 modules. Using these parameters, accumulative PV system is modeled in Matlab/Simulink, as shown in figure 4. Calculating total capacity of the system involves multiplying power rating of single module by the number of modules and parallel strings. This gives us a robust PV system having substantial energy output. Bypass diodes are also integrated strategically within modules to mitigate effects of shading. This addition further improves the reliability of PV system, particularly in scenarios where the occurrence of partial shading is more expected. There are several techniques for maximum power point tracking (MPPT) [23], [24], but the P&O method is the most widely used due to its simplicity and practicality. The algorithm is explained in detail in references [22] and [24]. Its function is to track the maximum current and voltage of the PV module with respect to changes in irradiance and temperature, in order to obtain the maximum power possible from the PV array.

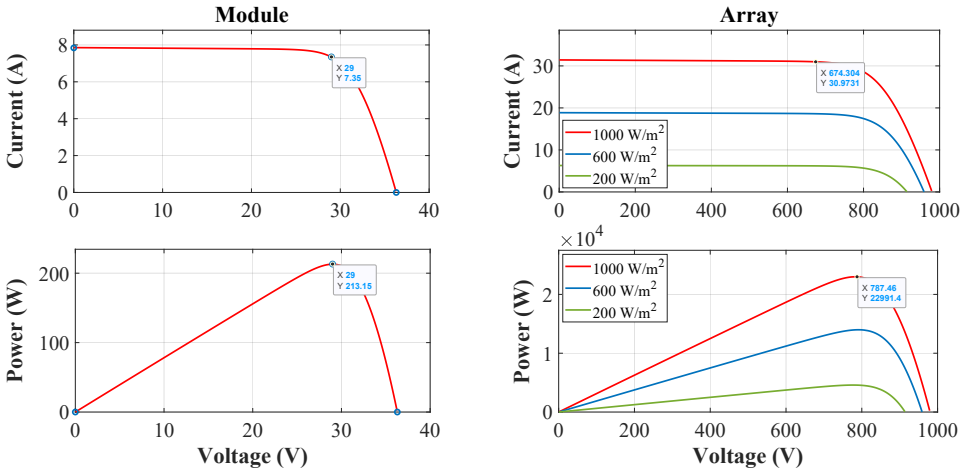

Figure 4: I-V and P-V characteristics of PV system.

C. Control of Microgrid system

The control strategy for a microgrid system is illustrated in Figure 5, that involves a two-stage three-phase grid-connected PV system. The first stage consists of a DC to DC converter that improves the utilization of the PV array and reduces the effects of shading. The second stage involves a three-phase VSI (DC/AC converter). The conventional control system is divided into two parts: inverter control and control of boost converter. The three-phase DC/AC inverter is composed of a dc-link voltage PI controller having feedback, a controller for power balancing, a phase-locked-loop (PLL) with a transformation module, (PI) proportional integral regulators [25], and coordinate DQ transformations.

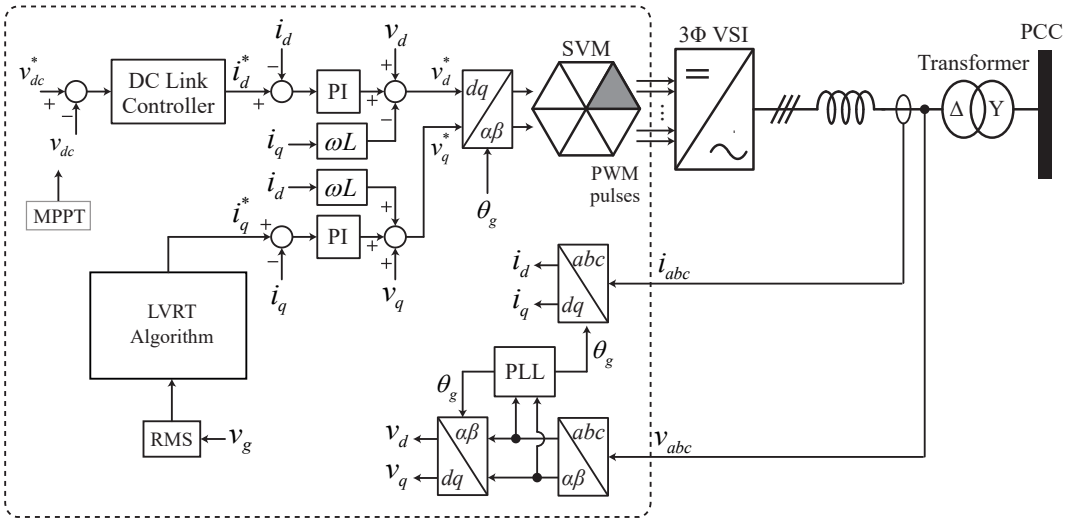

Figure 5: Grid-connected PV system Control structure.

1. Boost converter control

The primary purpose of a dc-dc boost converter is to obtain the highest power output from the PV panels, which typically fluctuates based on the amount of irradiation and temperature changes. The MPPT algorithm is employed to perform this function in conjunction with a proportional integral controller, which uses the dc-dc boost converter to track the anticipated maximum power point during normal microgrid operation.

2. VSI control

The VSI (Voltage Source Inverter) control is a technique used to regulate the output voltage of a DC-AC inverter. The VSI control usually consists of an outer voltage control loop and an inner current control loop. In this control scheme, a fixed reference value is compared to the DC-link voltage and then passed through a proportional-integral (PI) controller to generate a compensated reference current value, which forms the outer loop of the control system. The

Table 3: System parameters.

Parameters	Values	Parameters	Values
grid voltage	V_g = 25 kV	grid frequency	ω = 50 Hz
DC link voltage	V_{dc}=600 V	filter resistance	r_f = 1.25 Ω
filter inductance	L_f=2.5 mH	transformer	0.5/33 kV, 50 Hz
Current loop PI	K_p=0.3 , K_i=200	Voltage loop PI	K_p=2 , K_i=400

active current reference value (I_d^*) is obtained from the output of the voltage loop, while the reactive current reference value (I_q^*) is set to zero. In the inner loop of the control, injection of the current quality is performed by a current controller from the reference current value. Since a three-phase PV system can be implemented using a synchronous rotating reference frame, known to be DQ-Control, the injected grid current can be regulated using an orthogonal signal generator by a PI controller, as illustrated in figure 5. Finally, the injected current of the grid is synchronized with the grid voltage using a phase-locked-loop (PLL) system. To simplify the control of (I_d^*) and (I_q^*) currents, a feed-forward decoupling strategy [26] is used, and important parameters for the grid-connected inverter system are presented in Table 3. As previously mentioned, an SRF-PLL is used to synchronize the grid voltage and phase angle. This SRF-PLL produces θ, which is then used to transform from abc to dq0 frames.

The voltage equations for a grid inverter passing by an RL filter can be expressed as:

$$V_{ia} = L\frac{di_a}{dt} + Ri_a + v_{ga} \tag{5}$$

$$V_{ib} = L\frac{di_b}{dt} + Ri_b + v_{gb} \tag{6}$$

$$V_{ic} = L\frac{di_c}{dt} + Ri_c + v_{gc,} \tag{7}$$

where the variables (V_{ia}, V_{ib}, V_{ic}) represent inverter voltage, while (i_a, i_b, i_c) and (v_{ga}, v_{gb}, v_{gc}) indicate the inverter current and grid voltage, respectively. After transforming these variables into the dq reference frame, the equations are:

$$V_{id} = L\frac{di_d}{dt} + Ri_d + v_{gd} \tag{8}$$

$$V_{iq} = L\frac{di_q}{dt} + Ri_q + v_{gq} \tag{9}$$

$$P = \frac{3}{2}v_{gd}i_d \qquad and \qquad Q = -\frac{3}{2}v_{gd}i_q \tag{10}$$

Assuming that the system operates at unity power factor during normal operation, the losses can be neglected [26]. Therefore, the above given equations can be used to calculate active and reactive powers.

III. Low-Voltage Ride-Through (LVRT) Capability

One of the primary limitations of VSIs is their susceptibility to voltage fluctuations or disturbances. For instance, when there is a sudden voltage drop in the grid, the control mechanism responds by increasing the current to maintain a constant level of DC link voltage. Unfortunately, many of these voltage dips result from the propagation of various unbalanced faults within the grid. Undesirable power oscillations caused by such unbalanced voltages significantly disrupt the regulation of the DC link voltage. Consequently, the converter may trip to prevent any potential equipment damage caused by DC over-voltage.

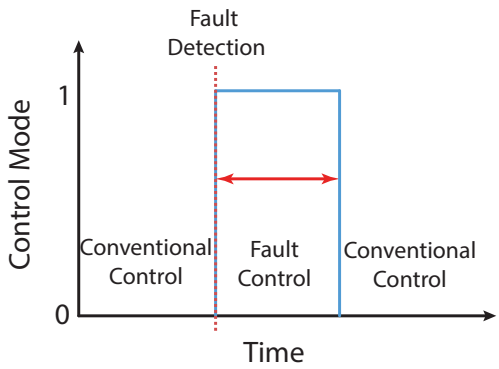

Figure 6: Control mode scheme.

Due to the occurrence of a fault, there is an imbalance between the power generated by the PV system and the power received by the grid, as previously explained. This imbalance results in over-voltage on the DC side and an excess of current on the AC side [27]. To safeguard electronic devices from undesirable current levels and over-voltage, a control method is employed, which includes a DC chopper circuit and a fault-current limiter. This control strategy, as designed, also contributes to the recovery of voltage during the fault period by injecting

reactive power in line with the degree of voltage sag. Figure 6 illustrates a simplified diagram depicting the transition between control modes. When a fault is detected, the value switches from 0 to 1, indicating normal or conventional control mode, after which the fault control mode is activated. The fault control mode operates for a specific duration, after which conventional control mode is reinstated. Once the voltage sag is identified, the chopper circuit becomes active to utilize the excess energy, and current limiter regulates any abnormal current [27]. These procedures maintain the microgrid system working in a stable condition and safeguard the power electronic equipment throughout the fault event.

A. Fault detection method

The primary function of LVRT control is to swiftly transition from normal operational mode to grid fault operational mode. Therefore, it is crucial to have a rapid and precise fault detection system or approach in place. Several fault detection methods have been identified in the past years, including the droop-control method [8], the missing voltage method [9], and the peak value detection method [7]. Among these, the Root Mean Square (RMS) method has emerged as highly effective and has gained widespread adoption in recent years.

The RMS fault detection method is much advantageous for its simplicity, effectiveness, and also real-time applicability. It does not require complex algorithms, which makes it suitable for rapid fault identification. RMS fault detection is capable of identifying various types of faults, that may include voltage sags, swells, harmonics, and also imbalances. This detection method is versatile, that allows for the detection of both transient as well as sustained faults. The RMS method is very often integrated in the protective relays and also monitoring systems. When the fault is detected, such systems can trigger protective measures like circuit breaker operations to isolate affected sections.

The RMS method used here for detecting voltage sags involves monitoring the root mean square value of the (dq) component of grid voltage at the Phase-Locked Loop (PLL) stage. This method computes the grid voltage at the current moment (referred to as V_{gp}) using the following equation:

$$V_{gp} = \sqrt{v_{gd}^2 + v_{gq}^2} \tag{11}$$

where v_{gd} and v_{gq} are the d and q component of the grid voltage, respectively.

B. Over-voltage control

During a fault, the electricity supplied to the grid falls significantly short of the power generated by the PV array. Consequently, there is an accumulation of higher voltage value at the DC link. This increase in the DC-link voltage causes the Maximum Power Point (MPP) to shift downward towards the open circuit voltage (V_{oc}), resulting in a reduction in the current output from the PV array. The deviation of the MPP during an event of fault can also lead to a delay in the restoration of normal values for PV current, voltage of PV, and the voltage at the DC-link point once the fault is cleared. To address this issue of over-voltage, DC chopper circuit [28] is incorporated into the system.

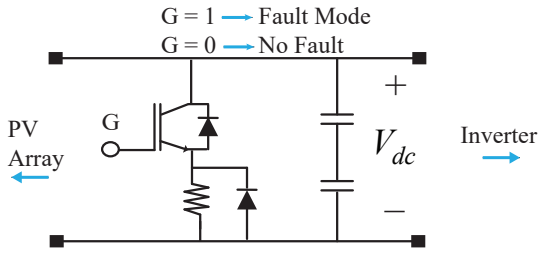

Figure 7: Dc chopper circuit.

Figure 7 illustrates a standard DC chopper circuit used to avert over-voltage

in the DC link. This DC chopper is essentially a protective circuit that operates in parallel with the DC-link capacitor. It comprises a resistor and an IGBT (Insulated Gate Bipolar Transistor), which is activated by a fault signal whenever the voltage surpasses a specific threshold level. The primary role of resistor is to stabilize the system with dissipating surplus power generated from the PV array. Additionally, a diode is connected in parallel with the resistor to mitigate any effects of stray inductance when the IGBT is off.

C. Excessive current limiting

Each PV-connected inverter within a grid system is designed with a specific limitation on the maximum AC current that it can handle. When a fault occurs, the AC current surpasses the maximum allowable limit for the inverter, resulting in the loss of connection from the grid. In response to fault, controller attempts to stabilize the grid voltage by decreasing the real power supplied to the grid. However, this action leads to an increase in the d-component of current, as observed in the SRF-PLL [1]. Since the inverter should inject reactive current during this voltage sag event, the q-component of current also rises. This increase in current components may trigger the inverter to disconnect from the system as a protective measure. To address this issue and ensure the inverter operates continuously and efficiently, a current value limiter is employed. This limiter helps maintain the current level within the acceptable range, enabling the inverter to function without interruption and resolve this problem.

D. Reactive current Injection

In order to support voltage restoration and offer assistance to the grid once a voltage sag is detected, an inverter needs to possess LVRT capability, which involves injecting reactive current. According to the regulations set forth by the

German grid codes [29], a PV microgrid system facing grid faults is required to supply a specific amount of reactive current, as depicted in Figure 8. German grid codes are basically regulatory standards that define technical requirements for connection and operation of power plants within the microgrid system. These codes address many aspects, that include the provision of reactive power/current support from the connected power plants. Reactive power/current injection plays a significant part in supporting and stabilizing the power systems. It helps manage the voltage levels, ensures efficient enough energy transfer, and contributes to reliability of the grid.

Reactive power/current injection becomes particularly very crucial during grid faults and/or disturbances. It contributes to maintain voltage levels and helps with the grid's recovery during situations/events like short circuits or very sudden load changes. These regulations specify that the system functions in normal mode of operation when the voltage amplitude (grid voltage) remains within the range of 0.9 per unit (p.u.) to 1.0 p.u. In such standard mode, the inverter injects only the active current. However, when the grid voltage drops below 0.9 p.u., the inverter must seamlessly switch to LVRT mode and possess the capability to provide reactive current in this state.

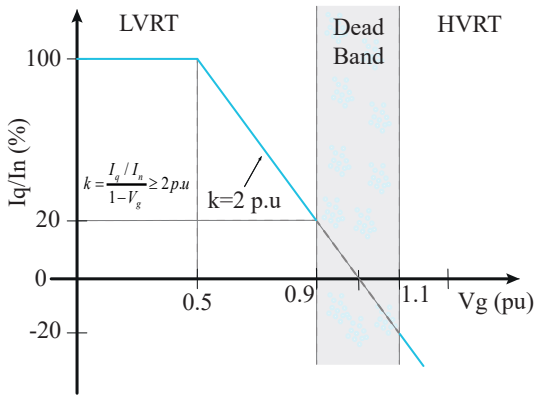

Figure 8: Required reactive current injection.

Following the stipulated grid regulations and taking into account the context provided in Figure 8, the required injection of reactive current can be expressed as follows:

$$\begin{aligned} i_q^* &= 0 \qquad if \qquad 1.1 \geq v_g > 0.9 \\ i_q^* &= k(1-v_g)I_n \qquad if \qquad 0.5 < v_g \leq 0.9 \\ i_q^* &= I_n \qquad if \qquad 0 \leq v_g \leq 0.5 \end{aligned}$$

where i_q^* is the value of injected reactive current, k is regarded as the droop constant ($k = 2$). v_g and I_n give grid voltage and rated current, respectively.

IV. Proposed NN-based LVRT Controller

Complex tasks demand a robust, resilient, and reliable controller for their proper execution. For instance, intricate responsibilities such as pattern recognition, system identification, classification, speech as well as vision processing, also control systems, require substantial computational power. A NN algorithm is basically a computational model that is inspired by the structure and also the function of human brain. It is used for tasks that may include pattern recognition, classification, regression, and also decision-making. Artificial Neural Networks (ANNs) have obtained substantial popularity in addressing these multifaceted challenges and solving a wide range of engineering problems [30].

The solution required by the neural network's computation is obtained by a process divided into three layers, namely; input layer, hidden layer and output layer. Input layer receives the data that contains data features. Main computation is performed in the hidden layer, where for each neuron weighted sum is calculated for the input value. Each input is multiplied by the corresponding weighted sum and a bias value is added to give flexibility to the model. After this, an activation function is applied to the computed weighted sum, which introduces non-linearity in the system enabling it to understand and learn complex relationships among the data. Finally the output layer gives the required solution that has been obtained by the undertaken learning process of the model. NN algorithm can be simply expressed as given in the equation 12.

$$Output = f(W \times Input + b) \tag{12}$$

where f is the activation function, W is the weights and b is the bias value.

ANNs are particularly suitable for predicting nonlinear parameters, like current in Grid-Connected Photovoltaic (GCPV) systems. The NN control method that is proposed in our work, which serves both the functions of grid

fault detection as well as injection of the required reactive current, is represented in the following Figure 9 along with the rest of the control.

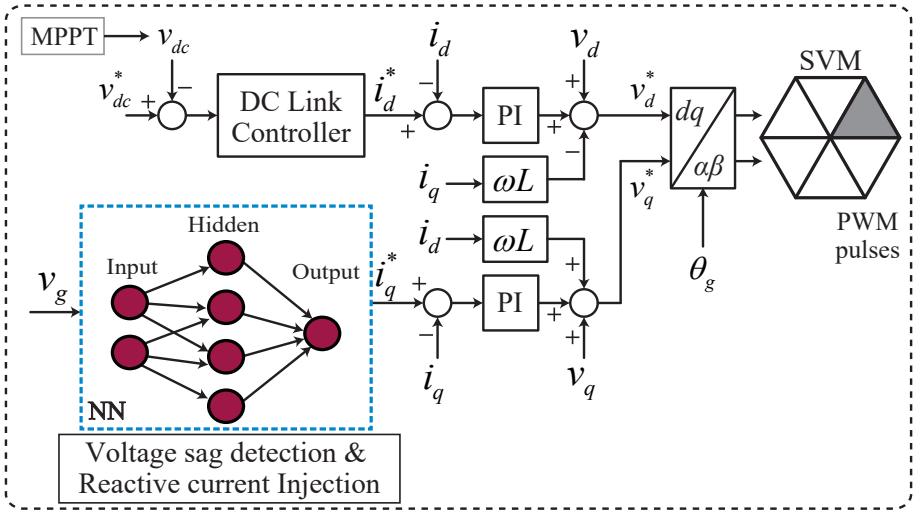

Figure 9: NN control structure.

A. Modelling a NN

Creating a neural network capable of performing both the functions of sag detection as well as reactive current injection requires several steps, which can be categorized as given next:

1. Data collection and Preprocessing

The first stage in constructing a neural network design entails collecting voltage, current, and pertinent parameter data values from the grid system. Subsequently, this data is subjected to cleaning and formatting processes, followed by normalization or scaling to ensure uniform input conditions. This phase also involves the selection of relevant features, the creation of new ones if necessary, and the correction of imbalances as needed. Through the organization and enhancement of the dataset, the neural network gains a deeper understanding of

the data and becomes more proficient at learning from it. This, in turn, results in a neural network model that is more accurate and dependable for the tasks of grid fault detection and the prediction of required reactive current injection.

2. Architecture of NN

The second phase entails assigning labels to the data collected, distinguishing between instances related to grid faults, labeled as ”fault,” and those representing normal operation, labeled as ”normal.” Following this, the dataset is partitioned into distinct training, validation, and testing subsets, which aids in the training and evaluation of the model. Subsequently, the architecture of the neural network as depicted in Figure 10(a) is designed. This architecture incorporates multiple layers, including an input layer with 2 neurons (representing voltage and/or current), hidden layers consisting 10 neurons for feature extraction, and an output layer having 1 neuron for both fault detection and the prediction of the required reactive current. This structural design is intended to capture intricate relationships within the data and empower the network for performing the dual tasks of grid faults detection and forecasting the necessary reactive current.

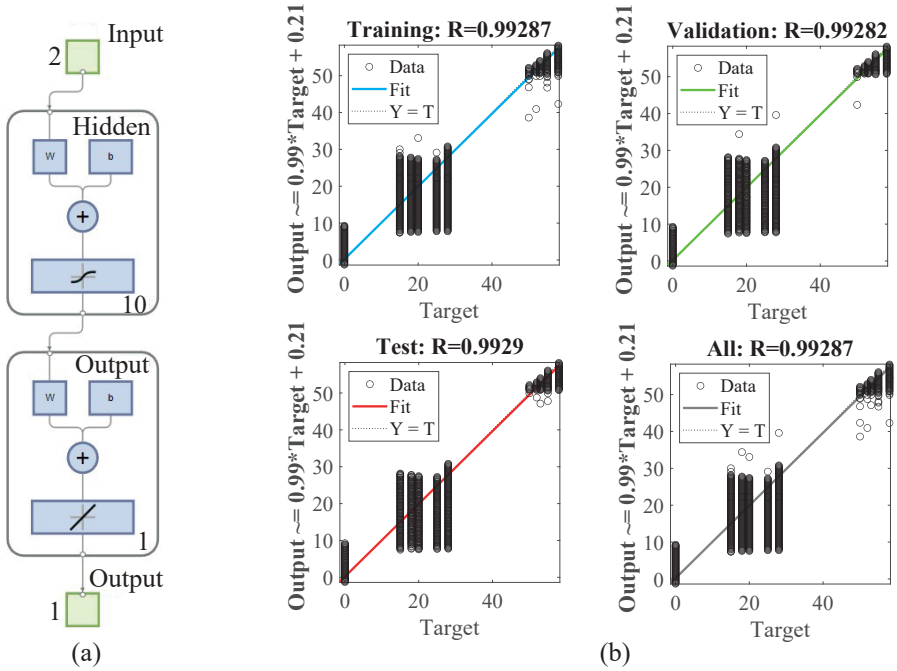

Figure 10: NN (a) Network structure, (b) Regression curve.

3. Training and Evaluation

In the third stage, the constructed NN undergoes training utilizing the labeled training dataset. The training process places particular emphasis on developing a precise loss function that takes into account both accuracy of fault detection and reactive current prediction accuracy. The NN's weights are adjusted iteratively with the help of back-propagation [31], and it's performance is continuously assessed using the validation dataset to avert overfitting. Upon evaluating the performance of the trained neural network, that achieving a high level of accuracy is characterized by the coefficient of correlation (R) approaching a value of 1 [32], while simultaneously minimizing mean squared error (MSE) to approach a value as near to 0 as possible. Subsequently, the trained NN is subjected to comprehensive evaluation using an independent testing dataset. This evaluation process includes the computation of performance metrics such as accuracy,

precision, recall, and mean absolute error, as depicted in Figure 11(a), for both fault detection as well as reactive current prediction. The results of this evaluation, illustrated in Figures 10(b) and 11(b), provide valuable insights to the model's effectiveness in simultaneously identifying grid faults and predicting the required reactive current accurately for system stabilization.

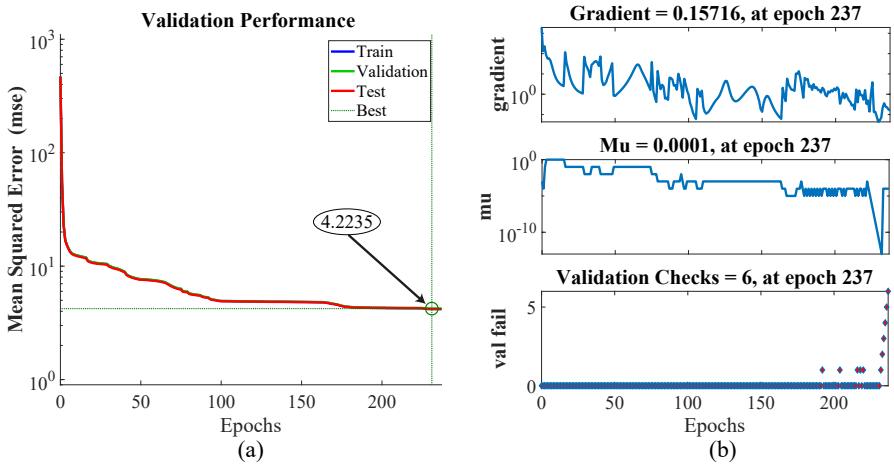

Figure 11: Evaluation of NN (a) MSE performance, (b) Training state.

4. Integration into the Grid

The last phase involves the incorporation of the trained neural network (NN) into the operational grid system, where it continuously collects real-time current and voltage data. Subsequently, the NN is applied to forecast grid faults and determine the necessary reactive current injections using this real-time data, enabling a prompt response to grid irregularities. Following this, performance of the model is consistently monitored and adjusted as necessary to ensure its ongoing reliability along with effectiveness. Ultimately, it is verified that the NN's predictions for reactive current injection align with the specified grid codes and regulations. This validation ensures that the predictions adhere to the required standards, contributing to the preservation of grid safety and stability.

B. NN-based LVRT control

The proposed neural network (NN) based control method plays a crucial role in improving grid reliability when voltage sags occur. Utilizing grid voltage (V_g) as its input, the NN not only identifies voltage sag occurrences but also evaluates their magnitude and duration. Importantly, it operates in alignment with grid code regulations, because of being trained to comprehend and adhere to such standards. This comprehensive approach enables the NN to make accurate predictions regarding the necessary reactive current injection (i_q^*) required to support the grid during dips, all while ensuring observance with regulatory constraints. The injection of this precisely calculated level of reactive power serves to stabilize the grid, mitigate the impacts of voltage sags, and maintain an uninterrupted power supply. This, in turn, strengthens the reliability and resilience of PV microgrid system, especially in changing and challenging grid conditions.

V. Results and Discussion

The PV-microgrid system, as depicted in Figure 2, has been set up in Simulink for the purpose of simulating and testing the proposed Low Voltage Ride Through (LVRT) control technique. This system is connected to a utility grid with a nominal voltage value of 25 kV. At the Point of Common Coupling (PCC), real-time measurements of current and voltage are continuously recorded. The designed system effectively manages AC current limitation and regulates the voltage at the DC-link, ensuring compliance with the specified requirements. As a result, the control system successfully maintains the connection of inverter during fault events and subsequently injects the necessary reactive current as determined by the proposed neural network (NN) model. In this section, we examine the behavior of the modeled PV-microgrid system when exposed to voltage sags, following the connection and protection of the inverter, while also ensuring the proper functioning of other equipment. All the results are obtained using the input parameters for the PV system, specifically a temperature (T) of 25 °C with irradiation (G) of 1000 W/m^2.

The testing process is divided into three specific cases, each representing a different sag scenario. The PV microgrid system's response to a three-phase-to-ground (L-L-L-G) fault occurring over a span of two seconds is evaluated under various sag conditions. It is analyzed that the system maintains its connectivity and can withstand voltage dips without experiencing any adverse stability issues. This ensures the proper functioning of the entire microgrid system, with the DC-link voltage also being controlled within acceptable limits.

A. Case 1

In the initial scenario, the grid was intentionally exposed to an 85% voltage sag to thoroughly evaluate how well the proposed control system would perform. The outcomes, as illustrated in Figure 12, demonstrate the grid voltage's response in

per unit (pu) values throughout the voltage sag, distinctly indicating when the sag occurred between 0.9 and 1.05 seconds.

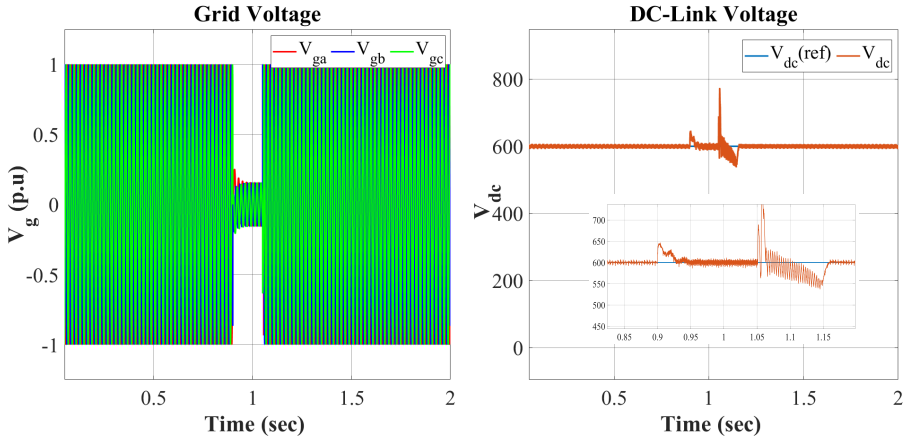

Figure 12: Grid and DC-link voltage with 85% sag.

Furthermore, it also presents the variations in the DC-link voltage during the voltage sag event. This dynamic analysis gives a more profound insight into how the DC-chopper circuit effectively maintained the stability of DC-link voltage within an acceptable range throughout the sag, which is a critical factor in upholding the overall stability of the system.

Figure 13 illustrates the comparison showing accuracy of fault detection between the RMS method and the proposed NN-based method. Despite a slightly slow convergence rate, the NN-based approach exhibited exceptional precision, stability and robustness in fault detection. On the otherhand, the RMS method showed minor delays in it's response, occasional overshooting, and undershooting, emphasizing the advantages of NN method, particularly in accurately detecting faults, even in challenging scenarios.

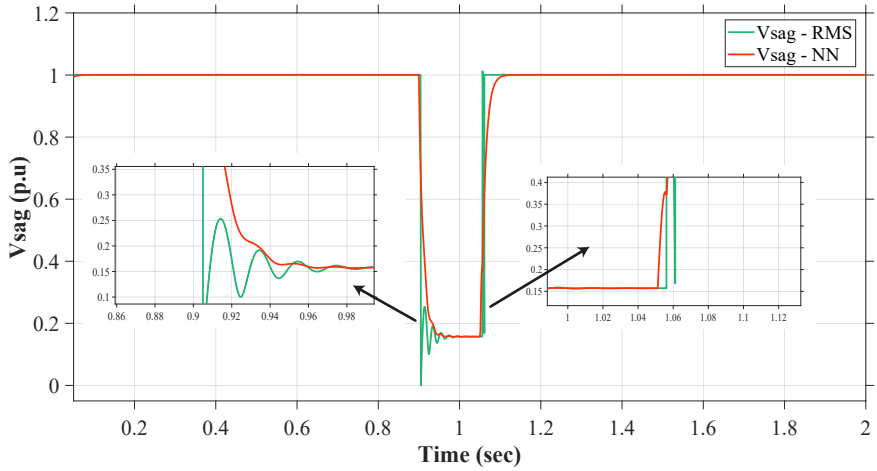

Figure 13: Detection of fault (85% sag).

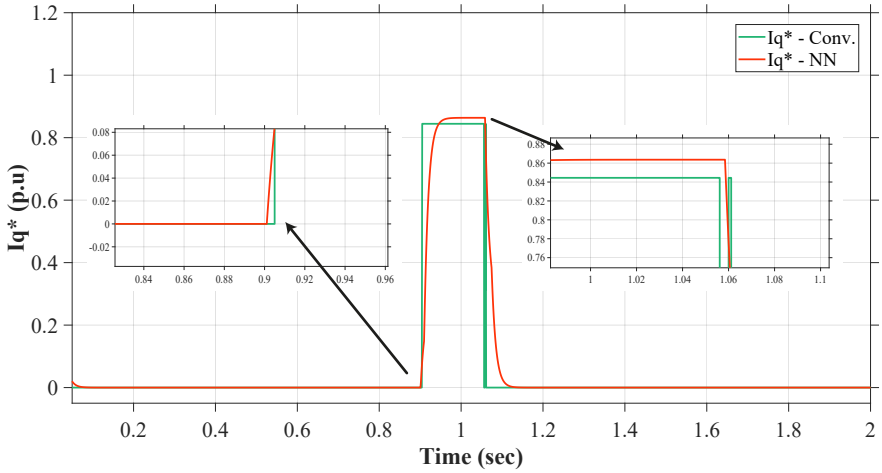

Figure 14: Reactive current injection (85% sag).

In regards to the reactive current injection, as depicted in the results obtained through simulation (Figure 14), the proposed NN-based control method demonstrated a significant improvement in terms of robustness and accuracy when compared to the conventional LVRT algorithm. Notably, the NN control method consistently and accurately responded to the injection of reactive current, highlighting its resilience in fulfilling the system's demands for reactive power. In contrast, the conventional LVRT algorithm exhibited slight delays in the injection

of reactive current and encountered stability issues during operation. This contrast underscores the superior performance and reliability of the NN-based control method in optimizing reactive current injection, proving it to be more promising and effective solution for maintaining stability of the grid.

B. Case 2

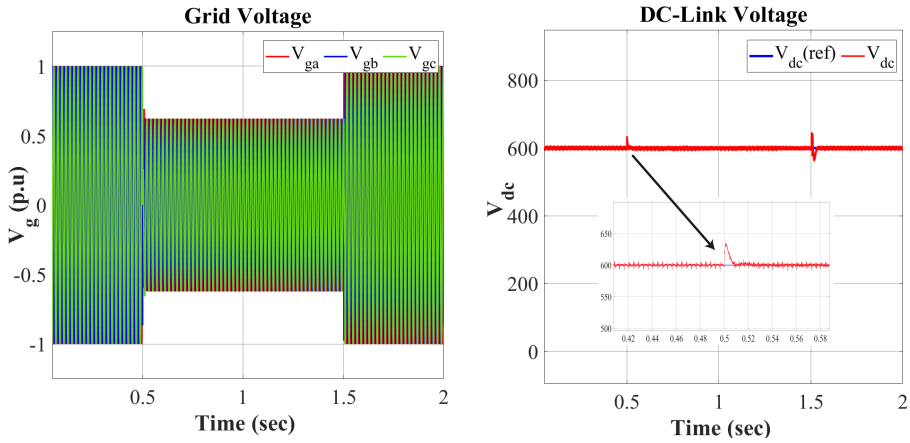

Figure 15: Grid and DC-link voltage with 38% sag.

The next case study delves into the response of grid voltage during the voltage sags, effectively showcasing the sag occurrence that spans from 0.5 seconds to 1.5 seconds. As depicted in Figure 15, DC-chopper circuit continues to excel in maintaining the stability of the DC-link voltage amidst the fluctuating grid voltage conditions, specifically during fault occurrences within the system.

Now, in the context of detecting voltage sag within this second scenario, which involves a fault of approximately 38%, the proposed NN-based control method remains consistent in its improvement of robustness and stability. Figure 16 highlights that the RMS method for fault detection encounters certain issues, particularly an undershoot at the time of occurrence of fault.

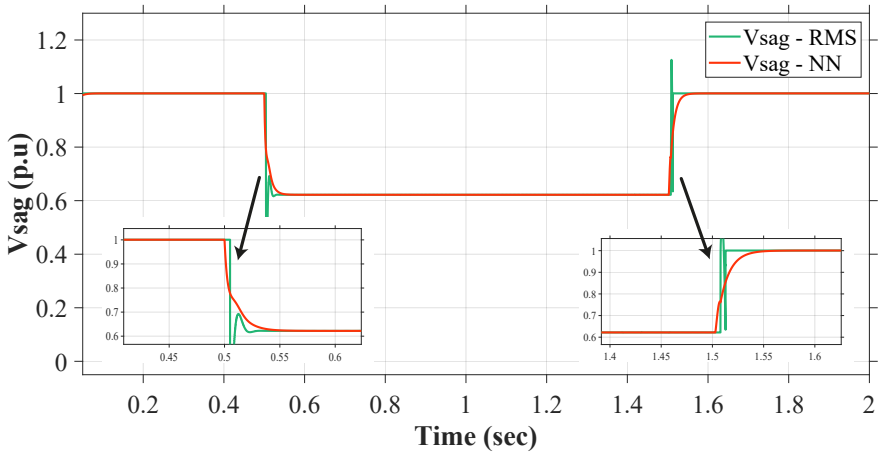

Figure 16: Detection of fault (38% sag).

This distorted sag detection signal introduces further instability into the system. Additionally, the overshoot during fault clearance in the RMS method can lead to irregular system behavior. Minor delays are observed in both cases of changing conditions, contributing to these shortcomings. Consequently, due to these drawbacks, required reactive current injection associated with this signal also exhibits instability and comparable drawbacks, as evident from Figure 17.

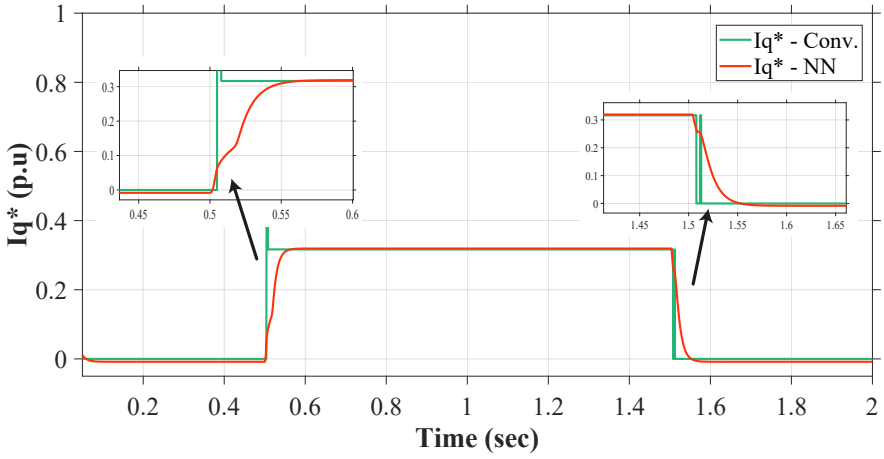

Figure 17: Reactive current injection (38% sag).

C. Case 3

In this third case study, simulation test was conducted over a duration of 2 seconds to scrutinize the system's performance under a complex fault scenario. Initially, a sag fault of 18% was introduced at the 0.5-second mark, persisting till 1.5 seconds. During this ongoing fault, another or additional fault of significantly higher magnitude occurred, that resulted in a combined fault magnitude of approx. 60% sag. This situation, featuring overlapping and concurrent sags, was employed to evaluate how effectively the proposed control system responded and exhibited resilience in such challenging circumstances. Once again, the DC-chopper circuit fulfilled its role by maintaining the DC-link voltage within acceptable limits, even in these demanding conditions. Figure 18 provides an overview of the DC-link voltage alongside the grid voltage during these overlapping conditions of fault.

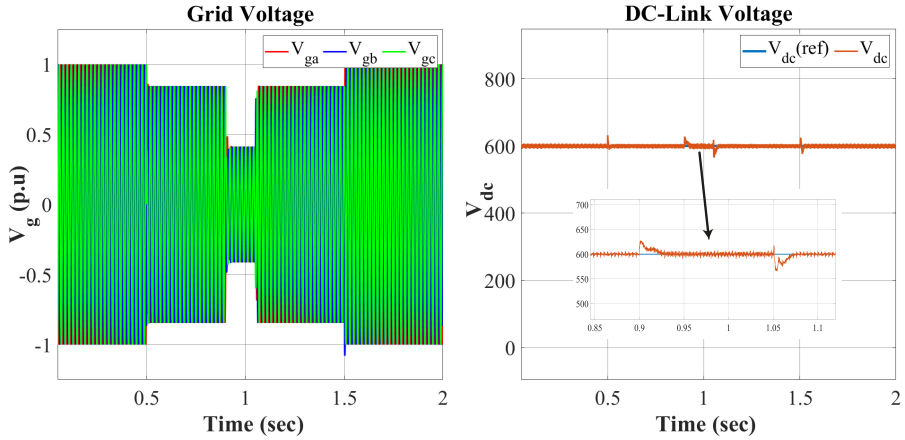

Figure 18: Grid and DC-link voltage with overlapping sags.

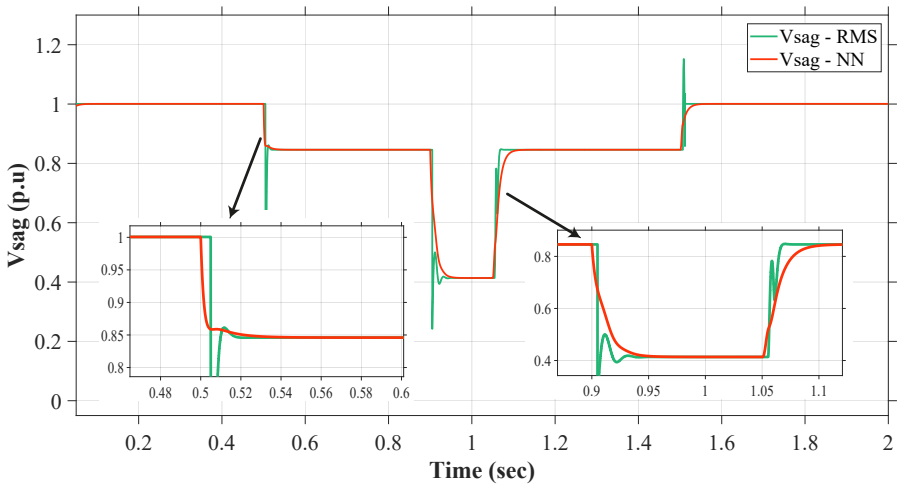

Figure 19: Detection of fault (overlapping sag).

The effectiveness of the created NN approach for detecting sags and injecting the required reactive current remained consistently superior, even in these challenging conditions, surpassing the performance of both the RMS and traditional LVRT methods. The visual representation of this comparative analysis describing sag detection and reactive current injection during the severe fault scenario is presented below as can be seen in Figures 19 and 20.

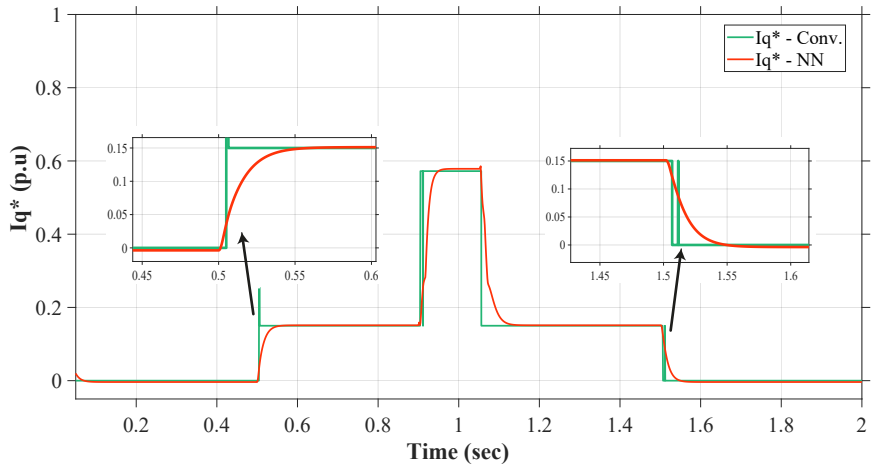

Figure 20: Reactive current injection (overlapping sag).

Table 4: Quantitative Analysis.

Parameters	**Conv. Method**	**NN Method**
Sag detection Delay	0.02s	0.001s
Current Injection Delay	0.05s	0.002s
Convergance Time	0.04s	0.03s
Undershoot at Sag detection	48.3%	0.0%
Overshoot at Current Injection	33.5%	0.0001%

The quantitative analysis that shows the comparative results between the conventional methods and proposed NN method for sag detection and required reactive current injection is given in table 4.

Figures 21 and 22 provide visual representations of the active and reactive currents traversing the system during these fault scenarios. Both of the modeled NN-based control and the conventional control approachs are employed for comparison. Additionally, these figures offer a more detailed scrutiny of the curve dynamics, enabling an examination of the control methods' transition behavior. Within this context, the proposed NN-based control method once again underscores its remarkable stability and resilience when confronted with intricate overlapping conditions of fault. Notably, the proposed NN method effectively mitigates overshooting and undershooting, delivering a smoother response in contrast to the less consistent performance exhibited by the conventional approach.

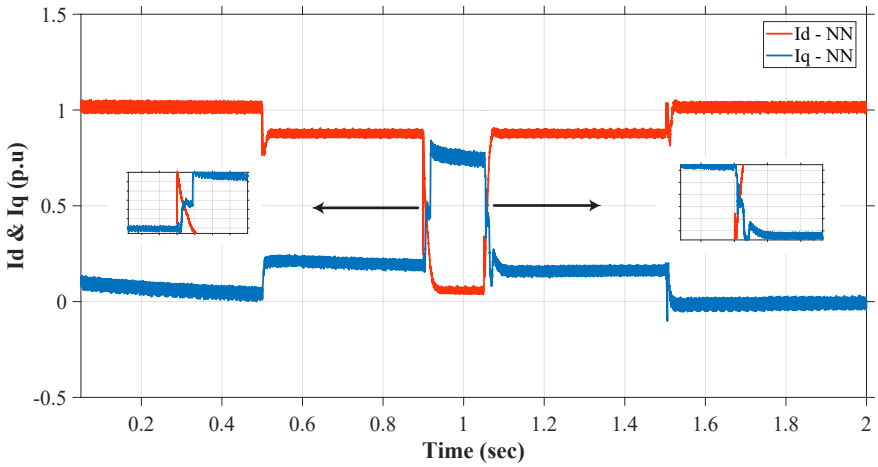

Figure 21: Active and reactive currents with NN-based control (overlapping sag).

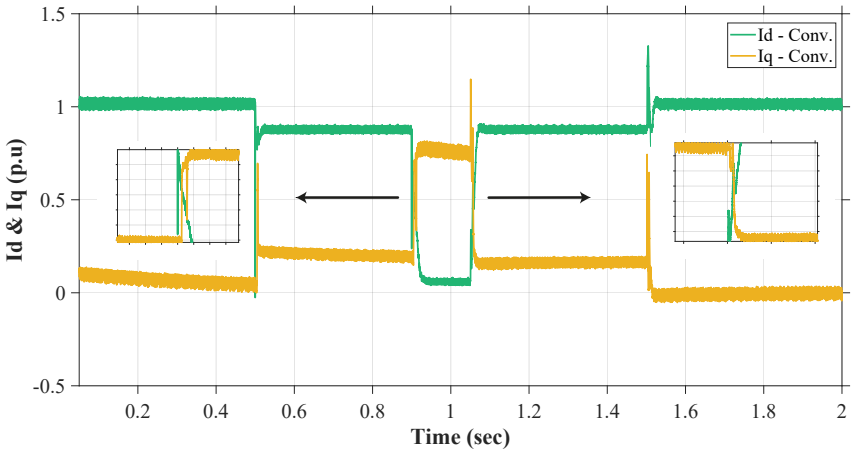

Figure 22: Active and reactive currents with conventional control (overlapping sag).

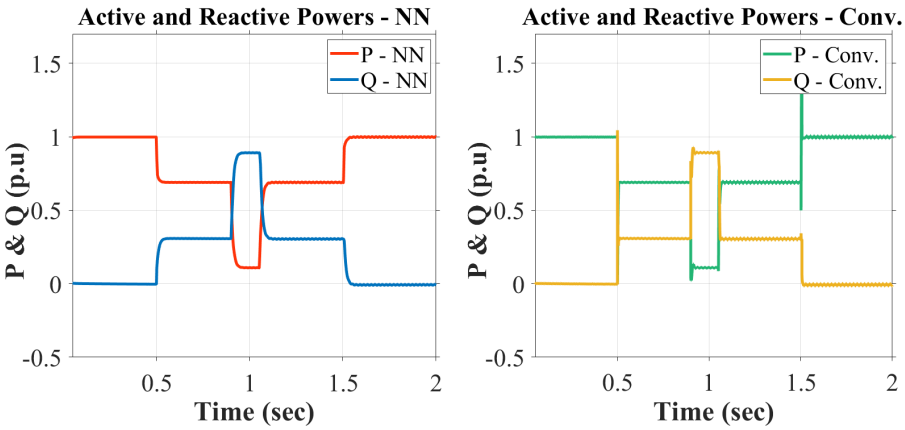

Figure 23: Active and reactive powers (overlapping sag).

In the end, Figure 23 presents the resulting dynamics of active and reactive powers in the system, employing both of the examined approaches. Undoubtedly, the sustained superiority of the proposed NN-based control system's outcomes is evident, underscoring its enduring resilience and stability, even when facing such severe sag conditions.

VI. CONCLUSION

In today's grid-connected power systems, there is a growing need to incorporate auxiliary services like uninterrupted power supplies and LVRT mechanisms for device protection. This work originates from an extensive study that culminated in the development of a LVRT control strategy tailored to effectively handle various grid failure situations and fault conditions. To address concerns related to DC-link over-voltage, DC-chopper circuit was employed. By harnessing the capabilities of the proposed NN-based control model, the system exhibited the ability to discern specific types of failures and promptly provide the required injections of reactive current to maintain stable and uninterrupted operations.

The seamless integration of the designed NN-based control model resulted in significant improvements within the photovoltaic (PV) microgrid system. These improvements encompassed more refined control methods, heightened resilience, increased system stability, reduced losses, and a more adaptable system architecture. The proficiency of the NN-based control model in mitigating voltage disruptions and supplying reactive power support through low-voltage fault scenarios played a pivotal role in ensuring the efficient and reliable operation of PV microgrid system. The development and evaluation of this work's system relied on cutting-edge technologies, underscoring the crucial role of innovative approaches in shaping contemporary power systems.

PUBLICATIONS

- Khan, M.A. and Kim, J. ”Smart Sag Detection and Reactive Current Injection Control for a PV Microgrid under Voltage Faults”. Energies 2023, 16,6776.

- Khan, M.A., Usama, M. and Kim, J. ”Integration of Renewable Energy Resources into DC Microgrids (Control and Protection) - a Review”. Renewable and Sustainable Energy Reviews. [Under Process].

REFERENCES

[1] J. Joshi, A. Swami, V. Jately, and B. Azzopardi, "A comprehensive review of control strategies to overcome challenges during lvrt in pv systems," *IEEE Access*, vol. 9, pp. 121 804–121 834, 2021.

[2] C. Tang, Y. Chen, and Y. Chen, "Pv power system with multi-mode operation and low-voltage ride-through capability," *IEEE Transactions on Industrial Electronics*, vol. 62, no. 12, pp. 7524–7533, 2015.

[3] A. A. Shetwi, M. Sujod, and F. Blaabjerg, "Low voltage ride-through capability control for single-stage inverter-based grid-connected photovoltaic power plant," *Solar Energy*, vol. 159, pp. 665–681, 2018.

[4] G. Ding, F. Gao, H. Tian, *et al.*, "Adaptive dc-link voltage control of two-stage photovoltaic inverter during low voltage ride-through operation," *IEEE Transactions on Power Electronics*, vol. 31, no. 6, pp. 4182–4194, 2016.

[5] D. Zeng, J. Guo, M. Ding, and D. Geng, "Fault ride-through capability enhancement by adaptive voltage support control for inverter interfaced distributed generation," in *5th International Conference on Electric Utility Deregulation and Restructuring and Power Technologies (DRPT)*, 2015.

[6] J. Miret, M. Castilla, A. Camacho, L. G. Vicuña, and J. Matas, "Control scheme for photovoltaic three-phase inverters to minimize peak currents during unbalanced grid-voltage sags," *IEEE Transactions on Power Electronics*, vol. 27, no. 10, pp. 4262–4271, 2012.

[7] Y. Yang, F. Blaabjerg, and Z. Zou, "Benchmarking of grid fault modes in single-phase grid-connected photovoltaic systems," *IEEE Transactions on Industry Applications*, vol. 49, pp. 2167–2176, 2013.

[8] J. Vasquez, R. Mastromauro, J. Guerrero, and M. Liserre, "Voltage support provided by a droop-controlled multifunctional inverter," *IEEE Transactions on Industrial Electronics*, vol. 56, pp. 4510–4519, 2009.

[9] K. Ding, K. Cheng, X. Xue, *et al.*, "A novel detection method for voltage sags," in *Proceedings of the 2nd International Conference on Power Electronics Systems and Applications*, Hong Kong, China.

[10] S. Silvestre, A. Chouder, and E. Karatepe, "Automatic fault detection in grid-connected pv systems," *Solar Energy*, vol. 94, pp. 119–127, 2013.

[11] S. Naderi, M. Negnevitsky, and K. Muttaqi, "A modified dc chopper for limiting the fault current and controlling the dc-link voltage to enhance fault ride-through capability of doubly-fed induction-generator-based wind turbine," *IEEE Transactions on Industry Applications*, vol. 55, pp. 2021–2032, 2019.

[12] A. Al-Durra, Y. Fayyad, S. Muyeen, and F. Blaabjerg, "Fault ride-through of a grid-connected photovoltaic system with quasi z source inverter," *Electric Power Components and Systems*, vol. 44, pp. 1786–1800, 2016.

[13] M. Islam, K. Muttaqi, and D. Sutanto, "A novel saturated amorphous alloy core based fault current limiter for improving the low voltage ride-through capability of doubly-fed induction generator-based wind turbines," *IEEE Transactions on Industry Applications*, vol. 57, pp. 2023–2034, 2021.

[14] D. Ramirez, S. Martinez, C. Platero, F. Blazquez, and R. de Castro, "Low-voltage ride-through capability for wind generators based on dynamic voltage restorers," *IEEE Transactions on Energy Conversion*, vol. 26, pp. 195–203, 2011.

[15] M. Döşoğlu, A. B. Arsoy, and U. Güvenç, "Application of statcom-supercapacitor for low-voltage ride-through capability in dfig-based wind farm," *Neural Computing and Applications*, vol. 28, pp. 2665–2674, 2016.

[16] A. Pal, D. Pal, and B. Panigrahi, "A current saturation strategy for enhancing the low voltage ride-through capability of grid-forming inverters," *IEEE Transactions on Circuits and Systems*, vol. 70, pp. 1009–1013, 2023.

[17] Y. Jiang, X. Li, C. Qin, X. Xing, and Z. Chen, "Improved particle swarm optimization based selective harmonic elimination and neutral point balance control for three-level inverter in low-voltage ride-through operation," *IEEE Transactions on Industrial Informatics*, vol. 18, pp. 642–652, 2022.

[18] X. Fu, S. Li, M. Fairbank, D. Wunsch, and E. Alonso, "Training recurrent neural networks with the levenberg-marquardt algorithm for optimal control of a grid-connected converter," *IEEE Transactions on Neural Networks and Learning Systems*, vol. 26, pp. 1900–1912, 2015.

[19] M. A. Khan and J. Kim, "Smart sag detection and reactive current injection control for a pv microgrid under voltage faults," *Energies*, vol. 16, p. 6776, 2023.

[20] A. Hussain, H. Sher, A. Murtaza, and K. Al-Hadeed, "Improved voltage controlled three-phase voltage source inverter using model predictive control for standalone system," in *Proceedings of the IECON (2018) - 44th Annual Conference of the IEEE Industrial Electronics Society*, Washington, DC, USA.

[21] A. Al-Shetwi and S. M. Zahim, "Modeling and simulation of photovoltaic module with enhanced perturb and observe mppt algorithm using matlab/simulink," *ARPN Journal of Engineering and Applied Sciences*, vol. 11, pp. 12 033–12 038, 2016.

[22] M. Villalva, J. Gazoli, and E. Filho, "Comprehensive approach to modeling and simulation of photovoltaic arrays," *IEEE Transactions on Power Electronics*, vol. 24, pp. 1198–1208, 2009.

[23] S. Saravanan and N. R. Babu, "Maximum power point tracking algorithms for photovoltaic system—a review," *Renewable and Sustainable Energy Reviews*, vol. 57, pp. 192–204, 2016.

[24] A. Durusu, I. Nakir, A. Ajder, R. Ayaz, H. Akca, and M. Tanrioven, "Performance comparison of widely-used maximum power point tracker algorithms under real environmental conditions," *Advances in Electrical and Computer Engineering*, vol. 14, pp. 89–94, 2014.

[25] M. Usama and J. Kim, "Low-speed transient and steady-state performance analysis of ipmsm for nonlinear speed regulator with effective compensation scheme," *Energies*, vol. 14, p. 6679, 2021.

[26] A. Azit, S. Sulaiman, Z. Hussein, *et al.*, "Tnb technical guidebook on grid-interconnection of photovoltaic power generation system to lv and mv networks," Tenaga Nasional Berhad, Kuala Lumpur, Malaysia, Tech. Rep., 2012, pp. 1–38.

[27] G. S. Islam, A. Al-Durra, S. Muyeen, and J. Tamura, "Low voltage ride through capability enhancement of grid connected large scale photovoltaic system," in *Proceedings of the IECON - 37th Annual Conference of the IEEE Industrial Electronics Society*, Melbourne, VIC, Australia.

[28] G. Pannell, B. Zahawi, D. Atkinson, and P. Missailidis, "Evaluation of the performance of a dc-link brake chopper as a dfig low-voltage fault-ride-through device," *IEEE Transactions on Energy Conversion*, vol. 28, pp. 535–542, 2013.

[29] T. Neumann and I. Erlich, "Modelling and control of photovoltaic inverter systems with respect to german grid code requirements," in *Proceedings of the IEEE Power and Energy Society General Meeting*, San Diego, CA, USA.

[30] Z. Hassan, A. Amir, J. Selvaraj, and N. Rahim, "A review on current injection techniques for low-voltage ride-through and grid fault conditions in grid-connected photovoltaic system," *Solar Energy*, pp. 851–873, 2020.

[31] A. Akpolat, M. Habibi, H. Baghaee, *et al.*, "Dynamic stabilization of dc microgrids using ann-based model predictive control," *IEEE Transactions on Energy Conversion*, vol. 37, pp. 999–1010, 2022.

[32] O. Okwako, Z. Lin, M. Xin, K. Premkumar, and A. Rodgers, "Neural network controlled solar pv battery powered unified power quality conditioner for grid connected operation," *Energies*, vol. 15, p. 6825, 2022.

ACKNOWLEDGEMENTS

I want to begin by offering all my praises to Allah the Almighty for blessing me with everything that has contributed to who I am today. I also want to extend my sincere appreciation to all those who have supported me throughout my research journey. Foremost among them is my advisor, Dr. Jaehong Kim, to whom I owe an immense debt of gratitude for his unwavering support during the past two years. His guidance, encouragement, and persistence have significantly influenced my approach to solving engineering problems. His extensive knowledge, tireless work ethic, and vast research experience, coupled with his remarkable patience in teaching, have been a constant source of inspiration and assistance in my journey toward developing critical thinking skills. I consider it a true privilege to have had the opportunity to study under his guidance.

I would also like to express my thanks to the members of my committee for their valuable contributions, feedback, and the time they dedicated to reviewing this thesis.